

# Polymer Brushes Patterned with Micrometer-Scale Chemical Gradients Using Laminar Co-Flow

Hyung-Jun Koo, Kristopher V. Waynant, Chunjie Zhang, and Paul V. Braun\*

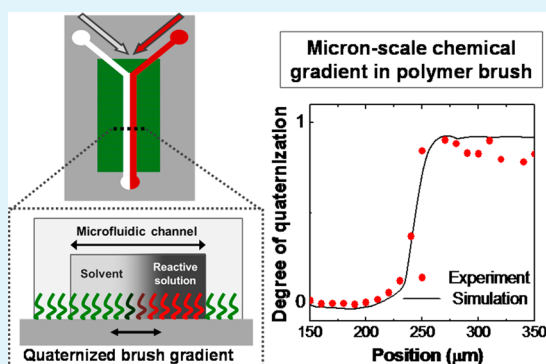
Department of Materials Science and Engineering, Beckman Institute for Advanced Science and Technology, and Frederick Seitz Materials Research Laboratory, University of Illinois at Urbana—Champaign, Urbana, Illinois 61801, United States

## S Supporting Information

**ABSTRACT:** We present a facile microfluidic method for forming narrow chemical gradients in polymer brushes. Co-flow of an alkylating agent solution and a neat solvent in a microfluidic channel forms a diffusion-driven concentration gradient, and thus a gradient in reaction rate at the interface of the two flows, leading to a quaternization gradient in the underlying poly(2-(dimethylamino)ethyl methacrylate) polymer brush. The spatial distribution of the quaternized polymer brush is characterized by confocal Raman microscopy. The quaternization gradient length in the polymer brush can be varied with the injection flow rate and the distance from the co-flow junction. A chemical gradient in the polymer brush as narrow as 5  $\mu\text{m}$  was created by controlling these parameters. The chemical gradient by laminar co-flow is compared with numerical calculations that include only one adjustable parameter: the

reaction rate constant of the polymer brush quaternization. The calculated chemical gradient agrees with the experimental data, which validates the numerical procedures established in this study. Flow of multiple laminar streams of reactive agent solutions enables single-run fabrication of brush gradients with more than one chemical property. As one example, four laminar streams—neat solvent/benzyl bromide solution/propargyl bromide solution/neat solvent—generate multistep gradients of aromatic and alkyne groups. Because the alkyne functional group is a click-reaction available site, the alkyne gradient could allow small gradient formation with a wide variety of chemical properties in a polymer brush.

**KEYWORDS:** polymer brush, chemical gradient, microfluidics, laminar flow, amine alkylation, click reaction



## INTRODUCTION

Surface-bound chemical gradients have been investigated for modulating cell behaviors, for high-throughput screening of biomolecules, and for chemical potential gradient driven transport of molecules and liquids.<sup>1</sup> Numerous top-down and bottom-up approaches to form surface gradients have been reported. However, formation and precise control of chemical gradients with length scales between a few micrometers and a few hundred micrometers remain challenging. One of the most effective techniques for creating short-period chemical gradients is laminar flow in a microfluidic device.<sup>2</sup> Due to the absence of turbulent mixing at low Reynolds numbers, the interface(s) between two or more miscible laminar flow streams becomes a diffusion-driven gradient in concentration. This well-defined concentration gradient has been used as is to generate a temporary dynamic physicochemical gradient, for example for studies of chemotaxis.<sup>3–6</sup> The concentration gradient can also be transferred onto a surface by flowing laminar streams containing various reactive agents<sup>2</sup> or depositable materials,<sup>7–10</sup> forming a static gradient on the bottom substrate. While this approach has been used to form physically/chemically graded solid surfaces, prior to our work here, it has not been demonstrated to form a few micron-scale gradients in polymer brushes.

Polymer brushes, polymer chain assemblies tethered to a solid substrate, provide mechanically and chemically stable functional thin films.<sup>11</sup> Through now well-established synthetic procedures, various types of highly dense functional groups can be realized in the polymer brush. Using an approach we termed DRAPE (Diffusion of Reactive Agent into PERmeable media), which was based on the diffusion and reaction of reactants into a PDMS slab surrounding a microfluidic channel, we formed 100–500  $\mu\text{m}$  lateral chemical gradients in polymer brushes.<sup>12</sup> The DRAPE method is simple and reliable, but neither multiple chemical gradients nor gradients on the order of a few micrometers length scale can be formed by this method. Here, we present a facile method for the formation of a sharp chemical gradient in a polymer brush via spatially selective postmodification using multiple laminar streams in a microfluidic channel. For example, to form a single gradient, an alkylating agent (benzyl bromide) containing solution and a nonreactive neat solvent are injected into the two arms of a Y-shaped microfluidic channel, forming a concentration gradient of the reactive agent at the interface of the co-flow (Figure 1a).

Received: June 7, 2014

Accepted: June 24, 2014

Published: June 24, 2014

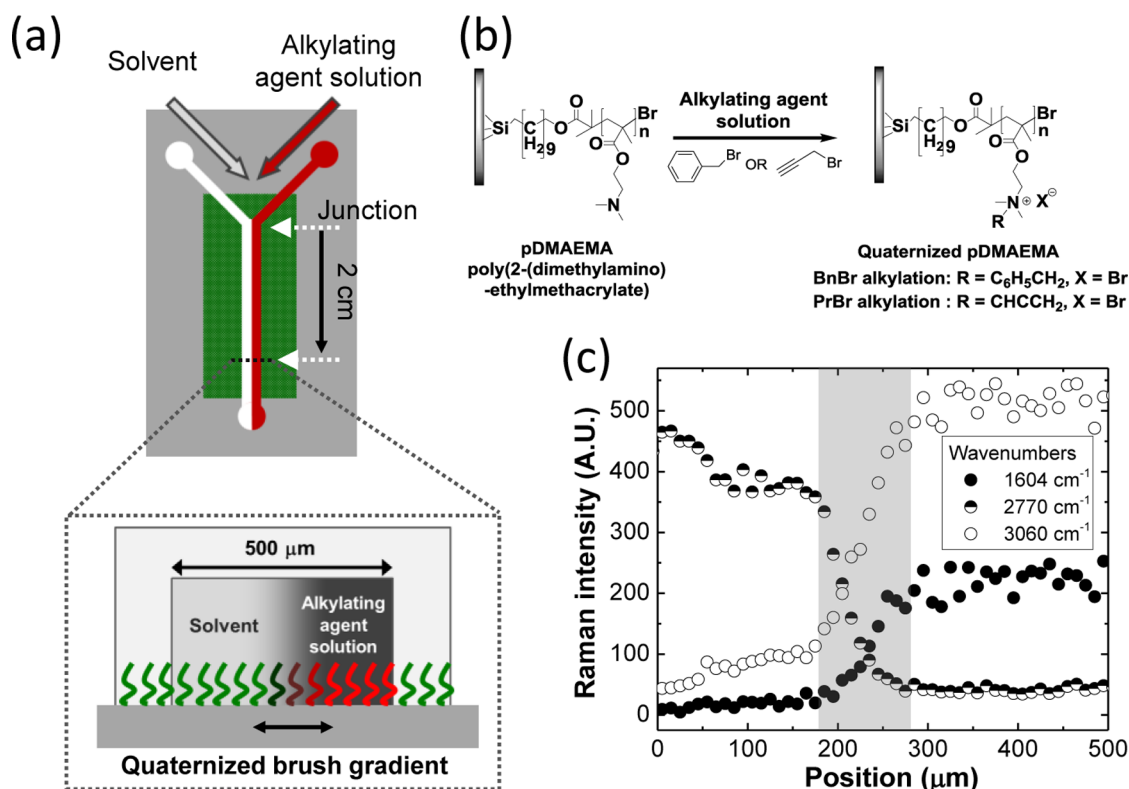


**Figure 1.** (a) Schematic illustration of the laminar flow-based polymer brush gradient formation. (b) Alkylation reactions of pDMAEMA by the two alkylating agents used in this study. (c) Raman intensity profiles of the peaks at 1604, 2770, and 3060  $\text{cm}^{-1}$  of the spectra collected across the gradient 2 cm downstream of the junction (Figure S1b, Supporting Information) as a function of a lateral position. The gradient was created by the co-flow of BnBr solution and neat solvent. The gray band indicates the expected gradient position.

The concentration gradient of the alkylating agent results in a quaternization gradient in the underlying polymer brush. The dependence of the resulting gradient length in the polymer brush on the injection flow rate and the distance from the Y-junction is investigated. A sharp quaternization gradient in the polymer brush as small as 5  $\mu\text{m}$  is formed by using laminar co-flow at a high injection rate. A numerical procedure to predict the quaternization gradient in the polymer brush is established by incorporating the simulated concentration distribution of the reactive agent in the laminar co-flow with reaction kinetics of the polymer quaternization. The well-defined laminar flows enable the formation of more than one quaternization gradient in a polymer brush with a single treatment. Of particular interest for forming a wide diversity of gradients, an alkyne functional group gradient amenable to click chemistry was formed in a polymer brush via quaternization by propargyl bromide. Multistep chemical gradients with more than one chemical property are formed by the use of two different alkylating agents followed by selective modification by click chemistry.

## EXPERIMENTAL SECTION

**pDMAEMA Brush Synthesis.** The poly(2-(dimethylamino)ethyl methacrylate) (pDMAEMA) brush was grown on a silicon wafer via surface-initiated atom transfer radical polymerization (SI-ATRP). Silicon wafers were cleaned in Nano-Strip (Cyantek) at 75 °C for 30 min, followed by washing with deionized water (Milli-Q Biocell System,  $R \geq 18 \text{ M}\Omega\text{-cm}$ ) and drying in a nitrogen flow. The initiator, (11-(2-bromo-2-methyl)propionyloxy)undecyltri-chlorosilane, synthesized as previously reported,<sup>13</sup> was printed on the cleaned wafers (single side polished; p-type; thickness, 356–406  $\mu\text{m}$ ; resistivity, 0.01–0.02  $\Omega\text{-cm}$ ; WRS Materials) via  $\mu$ -contact of an inked flat

polydimethylsiloxane (PDMS) stamp (areal dimension about 1.5  $\times$  3 cm). A 0.5% (v/v) initiator solution in hexane was used for stamping. The substrates with preprinted initiators were placed in a reaction vessel and purged. Separately, DMAEMA (7.07 g, 45 mmol, Sigma-Aldrich), removed of inhibitor, was diluted with 30 mL of deionized water and 15 mL of isopropyl alcohol, and the solution was degassed for at least 30 min. The solution was then added to a Schlenk flask under a positive nitrogen flow. 1,1,4,7,10,10-Hexamethyltriethylenetetramine as the ligand (122  $\mu\text{L}$ , 0.45 mmol, Sigma-Aldrich), CuBr (64.5 mg, 0.45 mmol, Sigma-Aldrich), and CuBr<sub>2</sub> (10 mg, 0.045 mmol, Sigma-Aldrich) were added to the DMAEMA solution, and the mixture was sealed. The solution of the monomer, catalyst, and ligand was transferred via cannula into the reaction vessel containing the substrates with the preprinted initiator. After 10 h, the substrates were removed, rinsed with isopropyl alcohol and deionized water, and dried in a nitrogen flow. The dry thickness of the grown polymer brush measured by ellipsometry and atomic force microscopy (AFM) in air varied between 70 and 100 nm.

**Fabrication of PDMS Microfluidic Channels.** The channel mold was prepared by spin-coating SU-8 photoresist polymer (2050, MicroChem, Inc.) on a silicon wafer. The resulting SU-8 film thickness after soft bake was  $\sim 75 \mu\text{m}$ . The photomask with a transparent channel pattern was placed on top of the baked SU-8 film and exposed to UV light (IntelliRay 400W) for 8 s at 80% of maximum intensity (Uvitron International, Inc.). After the post-exposure baking period, the SU-8 channel pattern was developed by rinsing with propylene glycol monomethyl ether acetate (Sigma-Aldrich). The precured PDMS (Sylgard 184 silicone elastomer kit; monomer base/curing agent = 10:1 in mass ratio; Dow Corning Corp.) was poured on the SU-8 pattern and cured at 75 °C for 90 min. The cured PDMS was peeled off, and holes at the channel ends were punched for connecting the inlet and outlet tubes.

**Microfluidic Setup for Gradient Formation in Polymer Brushes.** The schematic in Figure 1a illustrates the microfluidic

setup used for forming a chemical gradient in the polymer brush. The PDMS slab with the embedded Y-shaped microfluidic channel was placed on top of the pDMAEMA brush grown on a silicon wafer. The width and height of the microfluidic channel were 500 and 75  $\mu\text{m}$ , respectively. The PDMS slab and the silicon wafer with the surface-grown polymer brush were sandwiched between polycarbonate supports and clamped. The reactive agent solution and neat solvent without reactive agent were injected into two different inlets of the Y-shaped channel with a syringe pump (New Era Pump Systems, Inc.). The injection rate of each flow varied from 2 to 50  $\mu\text{L}/\text{min}$ . The two fluids flowing in the channel formed a laminar interface, where the diffusion-induced concentration gradient of the reactive agent was developed. Two different alkylating agents, benzyl bromide (BnBr, Sigma-Aldrich) and propargyl bromide (PrBr, Sigma-Aldrich), were used as the reactive agents for the study (Figure 1b). Both molecules quaternize the tertiary amine functional groups of the pDMAEMA brush. Because the reaction rate of the quaternization of the polymer brush is proportional to the concentration of the alkylating agent, the concentration gradient of the alkylating agent at the laminar interface(s) creates a quaternization gradient, and thus a charge gradient, in the underlying polymer brush. Unless otherwise mentioned, BnBr, which provides positive charge and adds aromaticity to the quaternized pDMAEMA brush,<sup>12</sup> was used as the alkylating agent. After gradient formation, the PDMS channel was removed from the polymer brush-coated substrate, and the substrate was quickly washed consecutively with isopropyl alcohol and water.

**Click-Reaction.** The pDMAEMA brush with the alkyne functional group was placed in 30 mL of nitrogen purged dimethylformamide (DMF) in a Schlenk flask. Methoxypolyethylene glycol azide (25 mg,  $M_n$  2000, Sigma-Aldrich), CuBr (5 mg, Sigma-Aldrich), and  $N,N,N',N',N''$ -pentamethyldiethylenetriamine (PMDETA, 5  $\mu\text{L}$ , Sigma-Aldrich) were dissolved in the DMF solvent. The solution was degassed by three freeze–pump–thaw cycles, and then reacted and stirred under nitrogen at room temperature for 20 h. After the reaction, the substrate was rinsed with isopropyl alcohol and deionized water and dried in a nitrogen flow.

## RESULTS AND DISCUSSION

**Gradient Characterization.** The chemical gradient in the polymer brush was characterized using confocal Raman spectroscopy. First, Raman spectra of the pDMAEMA brushes before and after the BnBr treatment are compared to determine the peaks characteristic to the quaternization (Figure S1a Supporting Information). After the brush was treated with BnBr, the aliphatic C–H vibration at 2770  $\text{cm}^{-1}$  nearly disappears,<sup>12,14</sup> while peaks at 1604 and 3060  $\text{cm}^{-1}$  appear. The new peaks are associated with the aromatic ring chain vibration<sup>15</sup> and aromatic C–H stretching,<sup>16</sup> confirming binding of the benzyl group, and thereby the quaternization of the pDMAEMA by BnBr. The chemical gradient in the pDMAEMA brush was formed by the laminar co-flow of 0.25 M BnBr in dimethyl sulfoxide (DMSO) and neat DMSO in the Y-shaped microfluidic device. The injection rate of each flow was 10  $\mu\text{L}/\text{min}$  (a linear velocity of about 9 mm/s), and the treatment time was 5 min. Throughout this article, the “flow rate” value will mean the injection rate of individual fluids of a co-flow unless mentioned otherwise, and therefore, the total flow rate would be twice the “flow rate” in the Y channel. The gradient was characterized via scanning confocal Raman spectroscopy (Horiba LabRAM HR 3D, Horiba) using a 532 nm laser and a 0.5 NA 50 $\times$  objective. The minimum lateral and vertical resolutions under this confocal measurement condition are 0.65 and 4.3  $\mu\text{m}$ , respectively. Raman spectra of the gradient-formed polymer brushes were collected every 10  $\mu\text{m}$  in the direction perpendicular to the flow direction (Figure S1b Supporting Information). The peak intensity changes at the

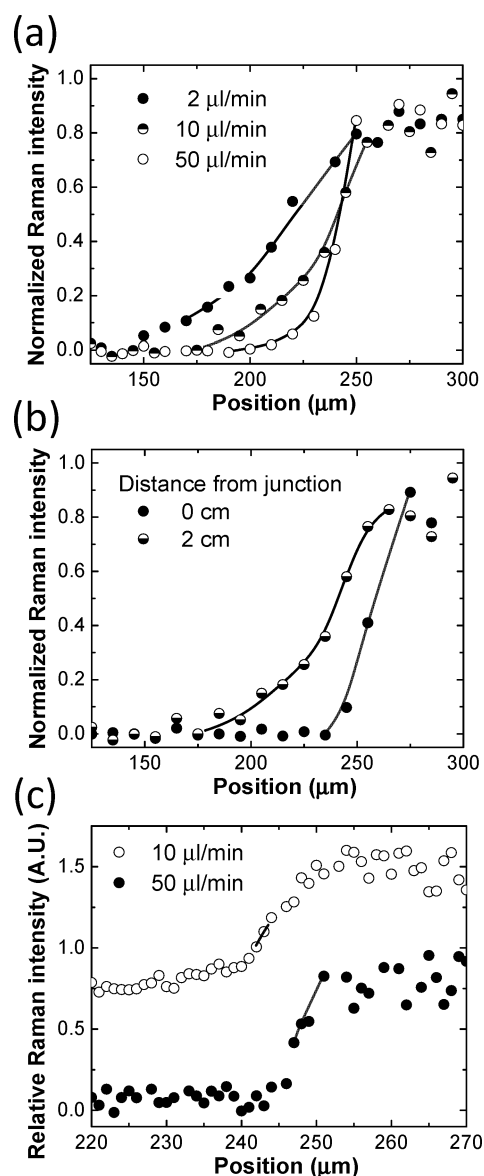


**Figure 2.** Raman intensity at 1604  $\text{cm}^{-1}$  as a function of (a) injection flow rates and (b) distance from the Y-junction. The Raman spectra for (a) were collected 2 cm away from the junction. The plots of (a) with the full x-axis range (0–500  $\mu\text{m}$ ) is shown in Figure S2 (Supporting Information). The flow rate in (b) is 10  $\mu\text{L}/\text{min}$ . (c) Recollected Raman intensity profile using a measurement interval of 1  $\mu\text{m}$  for the sharpest gradient in this study (formed at the Y-junction with 50  $\mu\text{L}/\text{min}$  individual flow rates). For all plots, the lines are visual guides.

characteristic wavenumbers of 1604, 2770, and 3060  $\text{cm}^{-1}$  are plotted in Figure 1c. The Raman intensity profiles of these characteristic peaks presumably represent the chemical (e.g., quaternization) gradient in the brush. The chemical gradient in the polymer brush is observed to be over  $\sim 100$   $\mu\text{m}$  on the basis of the spatial intensity changes of the characteristic peaks.

**Effect of Flow Rate and Distance from Y-Junction on the Gradient Length.** Because the concentration gradient results from the diffusion of the reactive molecules across the laminar co-flow interface, the gradient length increases as the co-flow residence time increases. Therefore, the length of the concentration gradient at the laminar co-flow interface is determined by both the flow rate and the distance from the Y-

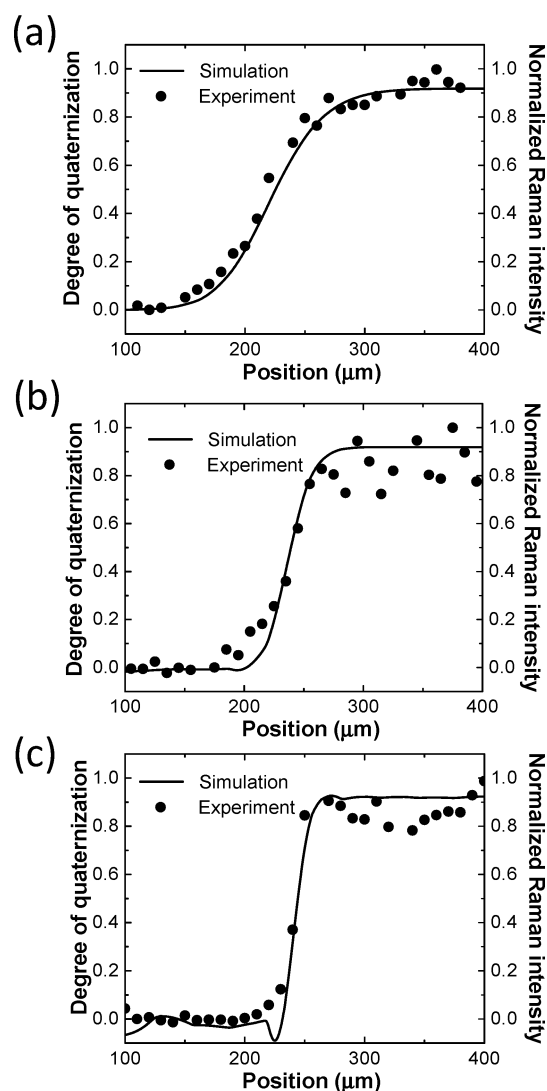


**Figure 3.** Comparison of simulated degree of quaternization and experimentally observed normalized Raman intensity at flow rates of (a) 2  $\mu\text{L}/\text{min}$ , (b) 10  $\mu\text{L}/\text{min}$ , and (c) 50  $\mu\text{L}/\text{min}$ . The unrealistic negative values of the degree of quaternization curve in (c) are due to the unstable simulation at the edge of the gradient at high flow rate (see Figure S7a, Supporting Information). The distance from the Y-junction for all data is 2 cm.

junction. The effect of the flow rate on the quaternization gradient length in the brush is shown in Figure 2a. The flow rate was varied from 2 to 50  $\mu\text{L}/\text{min}$ . The Raman peak intensity at 1601  $\text{cm}^{-1}$  is collected across the gradient 2 cm downstream of the junction (as in Figure 1c) and is normalized by the maximum peak intensity. The length of the quaternization gradient in the brush at 2 cm away from the Y-junction decreases from  $\sim 125$  to  $\sim 30$   $\mu\text{m}$  as the flow rate increases from 2 to 50  $\mu\text{L}/\text{min}$ . The decrease in the gradient length at higher flow rates is because the reactive agent molecules have less time to diffuse laterally into the solvent stream. Figure 2b shows the effect of the traveling distance of the co-flow on the gradient length, by comparing the gradient profiles formed at the Y-junction and at 2 cm away from the junction. The gradient length at the junction is less than 30  $\mu\text{m}$ , and expands to  $\sim 100$   $\mu\text{m}$  2 cm from the junction. The difference in the gradient length between the junction and 2 cm from the junction decreases as the flow rate increases (Figure

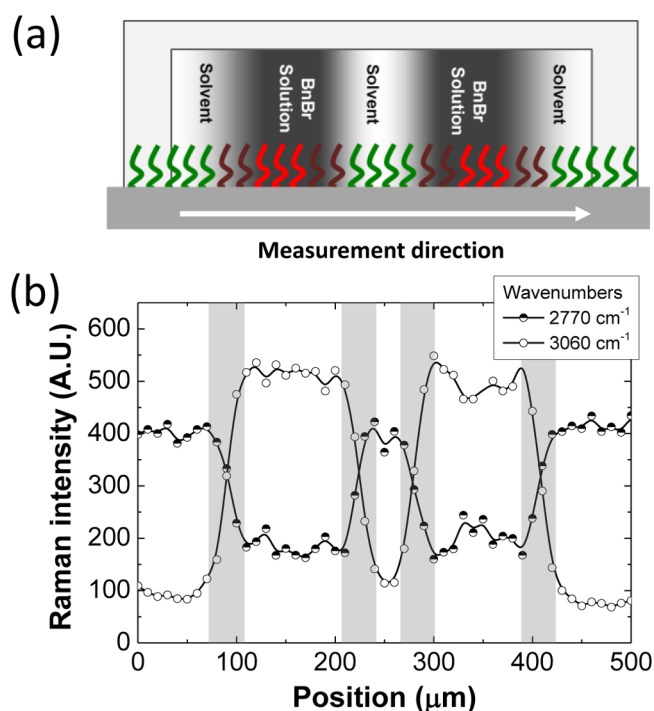


**Figure 4.** (a) Schematic of the formation of multiple chemical gradients using four parallel laminar interfaces. The white arrow indicates the measurement direction of the confocal Raman. (b) Raman intensity at 2770 and 3060  $\text{cm}^{-1}$  at the Y-junction. Raman intensity profiles of the peak at 2770  $\text{cm}^{-1}$  at the Y-junction and 2 cm downstream are compared in Figure S8 (Supporting Information). The injection rate of each flow is 10  $\mu\text{L}/\text{min}$ . The gray bands indicate the gradient positions. The lines are visual guides.

S3, Supporting Information), and at a high flow rate of 50  $\mu\text{L}/\text{min}$ , the gradient lengths at the junction and 2 cm from the junction are almost identical. Thus, the gradient length can be tuned by the flow rate and the distance from the Y-junction in the channel. Detailed characterization of the sharp gradient formed at the Y-junction with the highest flow rate of 50  $\mu\text{L}/\text{min}$  required a confocal Raman spot lateral spacing of 1  $\mu\text{m}$  rather than the 10  $\mu\text{m}$  lateral spacing normally used in this study. The recollected gradient profile in Figure 2c reveals that a gradient as narrow as  $\sim 5$   $\mu\text{m}$  is formed in the polymer brush by the reactive laminar co-flow. We would like to point out that forming such a tight gradient via a lithographic approach would require a rather sophisticated procedure. Here, such a gradient is formed via simple co-flow in a macroscopic microfluidic channel.

**Numerical Simulation of Chemical Gradients in Polymer Brush.** The experimental quaternization gradient in the polymer brush was compared with simulations to better understand the range of possible gradient lengths and strengths. Simulation details can be found in the Supporting Information. The polymer brush quaternization reaction is assumed to be second order overall, and thus, the degree of quaternization is calculated as follows,

$$\begin{aligned} \text{Degree of quaternization} &= 1 - \frac{[\text{brush}]_{\text{non-quaternized}}(\text{time} = t)}{[\text{brush}]_{\text{non-quaternized}}(\text{time} = 0)} \\ &= 1 - \exp(-k[\text{BnBr}] \cdot t) \end{aligned} \quad (1)$$

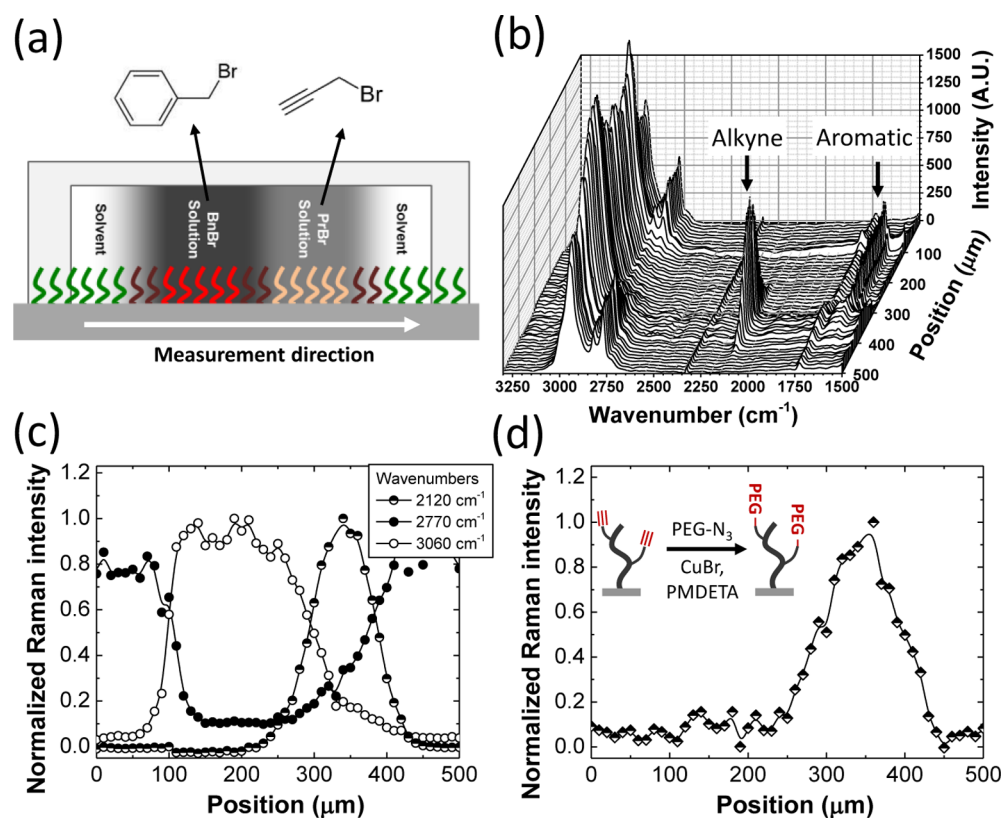


**Figure 5.** (a) Schematic illustration of the formation of the multistep gradient in a brush. The white arrow indicates the measurement direction of the confocal Raman spectroscope. (b) Confocal Raman spectra collected across the two-step gradient in polymer brushes at 1 cm from the Y-junction. (c) Normalized Raman peak intensity at 2120, 2770, and 3060  $\text{cm}^{-1}$  from the spectra in (b). (d) Normalized Raman intensity of the peak at 1930  $\text{cm}^{-1}$  corresponding to the PEG attachment after the click-reaction. (d, inset) Schematic of PEG attachment to the alkyne-functionalized polymer brush by click-reaction. The characteristic Raman peak at 1930  $\text{cm}^{-1}$  for the click-reaction of azide-functionalized PEG to pDMAEMA has been confirmed by comparing the Raman spectra of PrBr-quaternized pDMAEMA before and after the PEG click-reaction (Figure S10, Supporting Information). Raman spectra collected across the gradients after the click-reaction are shown in Figure S11 (Supporting Information).

where  $[\text{brush}]$  and  $[\text{BnBr}]$  are the concentrations of the polymer brush and the BnBr alkylating agent, respectively;  $k$  is the reaction rate constant of the quaternization reaction; and  $t$  is the quaternization reaction time. The reaction rate constant,  $k$ , was determined to be  $2 \text{ M}^{-1} \text{ min}^{-1}$  by fitting the rate of quaternization of the polymer brush at three different BnBr concentrations with eq 1 (Figures S4 and S5, Supporting Information). Then, the important input in eq 1, to estimate the quaternization gradient in the brush, is the BnBr concentration gradient profiles at the laminar co-flow interface in the microfluidic channel. This gradient profile was numerically simulated using COMSOL multiphysics (ver. 3.5) (see Figures S6 and S7a and details in the Supporting Information). With the reaction rate constant,  $k$ , and the reaction time,  $t$  (always 5 min in this study), the BnBr concentration profiles are then converted to quaternization profiles (Figure S7b, Supporting Information). Figure 3 compares the simulated quaternization profiles to the experimental results presented in Figure 2a. For all flow rates, the simulated gradient profiles are in excellent agreement with the experimental results. The established simulation procedure quantitatively predicts the quaternization profiles in the polymer brush.

**Multiple-Gradient Integration.** The well-defined nature of laminar flows enables the integration of more than one chemical gradient in the polymer brushes. To form multiple gradients, a microfluidic channel with five inlets was designed

(Figure S8a, Supporting Information), and the BnBr solution and the neat solvent were injected into alternate inlets. The five flow streams form four concentration gradients at the flow interfaces, as shown in Figure 4a, resulting in the multiple quaternization gradients in the polymer brush. The Raman intensities at 2770 and 3060  $\text{cm}^{-1}$  confirm the formation of the four  $\sim 30 \mu\text{m}$  long gradients in quaternization within the 500  $\mu\text{m}$  wide channel (Figure 4b). Multiple brush gradients with more than one chemistry can also be formed using multiple laminar flows with different reactive agents. Four laminar streams, DMSO/0.25 M BnBr in DMSO/0.1 M PrBr in DMSO/DMSO, form concentration gradients of BnBr and PrBr at the various stream interfaces, as shown in Figure 5a. Figure 5b displays the overlapped Raman spectra collected across the brush gradients. The peak newly appearing at 2120  $\text{cm}^{-1}$  results from the alkyne functional group bound to the amine group of pDMAEMA after the quaternization with PrBr.<sup>17,18</sup> This characteristic peak for the alkyne group was confirmed by comparing the Raman spectra of pDMAEMA brush before and after the PrBr treatment (Figure S9, Supporting Information). The normalized intensity change of the Raman peaks at 2120 and 3060  $\text{cm}^{-1}$  in Figure 5c shows that the consecutive gradients of alkyne and aromatic functional groups are successfully formed in the polymer brush. The Raman intensity of the peaks at 2770  $\text{cm}^{-1}$  is lower at the positions ranging between 70 and 430  $\mu\text{m}$ , which confirms the quaternization of the polymer brush by either BnBr or PrBr.<sup>14</sup>

The alkyne functional group bound to pDMAEMA is an available site for the azide–alkyne Huisgen cycloaddition, one of the most popular click-reactions,<sup>19,20</sup> allowing conversion of the alkyne group gradient to a variety of other chemistry gradients. As one example, hydrophilic polyethylene glycol-azide (PEG-N3) was attached to the alkyne functionalized polymer brush in Figure 5c via the click-reaction. Figure 5d shows the Raman peak intensity change at 1930 cm<sup>-1</sup>, the characteristic wavenumber for the azide–alkyne click-reaction (Figure S10, Supporting Information),<sup>21</sup> from the Raman spectra collected along the same measurement scanning line as Figure 5c. The peak intensity profile is in good accordance with that of the alkyne functional group in Figure 5c, revealing that the PEG is selectively attached to the alkyne sites of the pDMAEMA brush via the click-reaction. The characteristic peak at 2120 cm<sup>-1</sup> for the free alkyne functional group almost vanishes after the click-reaction (Figure S11, Supporting Information). PEG is a well-known cell repellent polymer, so this gradient surface could perhaps be used for surface-assisted cell haptotaxis.<sup>8</sup> The number of gradients is only limited by the number of reactive laminar streams, and because the chemistry of each stream can be different, this approach allows the formation of multiple gradients of diverse chemical properties in the polymer brush.

## CONCLUSION

We developed a facile and general method for the formation of well-defined narrow chemical gradients in polymer brushes by using laminar streams of multiple reactive agent solutions. The concentration gradient at the interface of the alkylating agent solution and the neat solvent leads to a quaternization gradient in the underlying neutral polymer brush. The resulting quaternization gradient can be precisely controlled by the injection flow rate and the distance from the junction where two streams of the reactive agent solution and the solvent first form an interface. A numerical procedure based on the reaction kinetics and the simulated concentration profiles in a microfluidic channel is established. The validity of the numerical procedure is verified by comparing the calculated gradient profiles with the experimental data. Multiple laminar flows of the reactive solutions allow the formation of the more than one chemical gradients in a small area of the polymer brush. The gradient of the alkyne functional group is formed by the laminar co-flow with PrBr solution and is converted to the PEG gradient via the subsequent click-reaction. This multistep gradient including alkyne groups further extends the available types of chemical gradients. The method is simple and reliable, and it should be generally applicable to other solution-based post-treatments (e.g., hydrolysis) to form other polymer brush gradients. Moreover, such a highly controllable method based on the laminar co-flow interface could enable integrating multiple gradients with various chemical properties, thereby fabricating a gradient assay with sophisticated configuration of dense variables or a gradient “circuit” for directed molecular transport.<sup>22</sup>

## ASSOCIATED CONTENT

### Supporting Information

Raman spectra before and after alkylation and click reaction, overlapped Raman spectra and Raman peak intensity profiles collected across various gradients, and detailed information on the numerical calculation and simulation procedure used to

calculate gradient profiles. This material is available free of charge via the Internet at <http://pubs.acs.org>.

## AUTHOR INFORMATION

### Corresponding Author

\*E-mail: [pbraun@illinois.edu](mailto:pbraun@illinois.edu).

### Notes

The authors declare no competing financial interest.

## ACKNOWLEDGMENTS

The work was supported by Defense Threat Reduction Agency under award number HDTRA 1-12-1-0035. The authors thank Dr. Brian Pate (DTRA) for helpful discussions.

## REFERENCES

- (1) Genzer, J.; Bhat, R. R. Surface-Bound Soft Matter Gradients. *Langmuir* **2008**, *24*, 2294–2317.
- (2) Jeon, N. L.; Dertinger, S. K. W.; Chiu, D. T.; Choi, I. S.; Stroock, A. D.; Whitesides, G. M. Generation of Solution and Surface Gradients Using Microfluidic Systems. *Langmuir* **2000**, *16*, 8311–8316.
- (3) Meier, B.; Zielinski, A.; Weber, C.; Arcizet, D.; Youssef, S.; Franosch, T.; Rädler, J. O.; Heinrich, D. Chemotactic Cell Trapping in Controlled Alternating Gradient Fields. *Proc. Natl. Acad. Sci. U.S.A.* **2011**, *108*, 11417–11422.
- (4) Chung, B. G.; Flanagan, L. A.; Rhee, S. W.; Schwartz, P. H.; Lee, A. P.; Monuki, E. S.; Jeon, N. L. Human Neural Stem Cell Growth and Differentiation in a Gradient-Generating Microfluidic Device. *Lab Chip* **2005**, *5*, 401–406.
- (5) Wu, J.; Wu, X.; Lin, F. Recent Developments in Microfluidics-Based Chemotaxis Studies. *Lab Chip* **2013**, *13*, 2484–2499.
- (6) Frank, T.; Tay, S. Flow-Switching Allows Independently Programmable, Extremely Stable, High-Throughput Diffusion-Based Gradients. *Lab Chip* **2013**, *13*, 1273–1281.
- (7) Kreppenhof, K.; Li, J.; Segura, R.; Popp, L.; Rossi, M.; Tzvetkova, P.; Luy, B.; Kähler, C. J.; Guber, A. E.; Levkin, P. A. Formation of a Polymer Surface with a Gradient of Pore Size Using a Microfluidic Chip. *Langmuir* **2013**, *29*, 3797–3804.
- (8) Burdick, J. A.; Khademhosseini, A.; Langer, R. Fabrication of Gradient Hydrogels Using a Microfluidics/Photopolymerization Process. *Langmuir* **2004**, *20*, 5153–5156.
- (9) Zaari, N.; Rajagopalan, P.; Kim, S. K.; Engler, A. J.; Wong, J. Y. Photopolymerization in Microfluidic Gradient Generators: Microscale Control of Substrate Compliance to Manipulate Cell Response. *Adv. Mater.* **2004**, *16*, 2133–2137.
- (10) Shi, X.; Ostrovidov, S.; Shu, Y.; Liang, X.; Nakajima, K.; Wu, H.; Khademhosseini, A. Microfluidic Generation of Polydopamine Gradients on Hydrophobic Surfaces. *Langmuir* **2013**.
- (11) Azzaroni, O. Polymer Brushes Here, There, and Everywhere: Recent Advances in Their Practical Applications and Emerging Opportunities in Multiple Research Fields. *J. Polym. Sci., Part A: Polym. Chem.* **2012**, *50*, 3225–3258.
- (12) Koo, H.-J.; Waynant, K. V.; Zhang, C.; Haasch, R. T.; Braun, P. V. General Method for Forming Micrometer-Scale Lateral Chemical Gradients in Polymer Brushes. *Chem. Mater.* **2014**, *26*, 2678–2683.
- (13) Matyjaszewski, K.; Miller, P. J.; Shukla, N.; Immaraporn, B.; Gelman, A.; Luokala, B. B.; Siclován, T. M.; Kickelbick, G.; Vallant, T.; Hoffmann, H.; Pakula, T. Polymers at Interfaces: Using Atom Transfer Radical Polymerization in the Controlled Growth of Homopolymers and Block Copolymers from Silicon Surfaces in the Absence of Untethered Sacrificial Initiator. *Macromolecules* **1999**, *32*, 8716–8724.
- (14) Sanjuan, S.; Perrin, P.; Pantoustier, N.; Tran, Y. Synthesis and Swelling Behavior of pH-Responsive Polybase Brushes. *Langmuir* **2007**, *23*, 5769–5778.
- (15) Roy, D.; Guthrie, J. T.; Perrier, S. Synthesis of Natural-Synthetic Hybrid Materials from Cellulose via the RAFT Process. *Soft Matter* **2008**, *4*, 145–155.

- (16) Bower, D. I.; Maddams, W. F. *The Vibrational Spectroscopy of Polymers*; Cambridge University Press: Cambridge, UK, 1989.
- (17) Kennedy, D. C.; McKay, C. S.; Tay, L.-I.; Rouleau, Y.; Pezacki, J. P. Carbon-Bonded Silver Nanoparticles: Alkyne-Functionalized Ligands for SERS Imaging of Mammalian Cells. *Chem. Commun.* **2011**, *47*, 3156–3158.
- (18) Yamakoshi, H.; Dodo, K.; Okada, M.; Ando, J.; Palonpon, A.; Fujita, K.; Kawata, S.; Sodeoka, M. Imaging of EdU, an Alkyne-Tagged Cell Proliferation Probe, by Raman Microscopy. *J. Am. Chem. Soc.* **2011**, *133*, 6102–6105.
- (19) Kolb, H. C.; Finn, M. G.; Sharpless, K. B. Click Chemistry: Diverse Chemical Function from a Few Good Reactions. *Angew. Chem., Int. Ed.* **2001**, *40*, 2004–2021.
- (20) Huisgen, R. 1,3-Dipolar Cycloadditions. *Proc. Chem. Soc.* **1961**, 357–396.
- (21) Breed, D. R.; Thibault, R.; Xie, F.; Wang, Q.; Hawker, C. J.; Pine, D. J. Functionalization of Polymer Microspheres Using Click Chemistry. *Langmuir* **2009**, *25*, 4370–4376.
- (22) Yonet-Tanyeri, N.; Evans, R. C.; Tu, H.; Braun, P. V. Molecular Transport Directed via Patterned Functionalized Surfaces. *Adv. Mater.* **2011**, *23*, 1739–1743.